ASM Sc. J., 12, Special Issue 4, 2019 for ICSE2018, 118-124

# Nanoparticle Optical Properties: Effect of Shell Thickness of Silica Core-Gold Nanoshell on Surface Plasmon Resonance

Norsyahidah Md Saleh[1] and Azlan Abdul Aziz[2]

*School of Physics, Universiti Sains Malaysia, 11800 USM Pulau Pinang, Pulau Pinang, Malaysia*

It has been widely shown that gold nanoparticle emission wavelength redshifted when the diameter of the gold nanoparticle increases. This redshift is universally dependent not only to nanoparticles' size but also on their shape, type of metal, or the environment dielectric constant. However, the latter contribution is extremely difficult to be characterize experimentally due to the complexity of synthesize and method of determining the thickness and dielectric constant of the shell. In this paper, we resolved those issues by calculating the extinction efficiency of dielectric core-metal nanoshell plasmon resonance nanostructure using silica and gold template respectively. The calculation was conducted using MATLAB toolbox on metallic nanoparticle using boundary element method (MNPBEM), deploying a full Maxwell's equation in this simulation of silica core-gold nanoshells. The total silica core-gold nanoshell diameter in defining the plasmon resonance was specifically analysed, determined from the coupling of the inner shell surface (cavity) and the outer shell surface (sphere) plasmons over a separation distance given by the gold nanoshell thickness, to be consistent with the published work on plasmon hybridization model. By using this silica-gold nanoshell, surface plasmon resonance was shown to achieve a higher wavelength position near infrared region. The hybridization of the outer shell-surface sphere mode and inner shell-surface sphere cavity mode reveal that gold nanoshell is more suitable to in-vivo imaging and therapy application as compared to gold nanosphere.

**Keywords:** MNPBEM, Silica core—gold nanoshell, Surface plasmon resonance

## I. INTRODUCTION

Gold nanoparticle is an excellent light scatters and absorbers at optical frequencies due to its strongly enhanced surface plasmon resonance. Those outstanding optical properties has also motivated interest in the use of plasmon-resonant nanoparticles and nanostructures for optical and photonic applications [4], [5] and the most recent research for biomedical applications [6], [7], [16]–[18], [8]–[15]. Gold nanoparticle also have good biocompatibility with facile synthesis [19], making it material of choice for the use in biochemical sensing and detection, medical diagnostics and therapeutic applications. The experimental reports on the optical properties of gold nanoparticles on nanospheres, nanoshell and nanorods have been well documented [2], [20]–[28]. Some of these work focused on the unique optical tenability of dielectric core-metal shell nanostructure which consist of silica core encapsulated with a few nanometer thin gold layer. It is found to be strongly dependent on the relative dimensions of the gold shell and dielectric silica core. By decreasing experimentally the shell thickness, the plasmon band was shown to be redshifted to near infrared region. Since biological tissue shows maximum optical transmissivity in the 650-900 nm region, the wavelength redshift of silica core gold nanoshell structure can be very useful in

[1] corresponding author: syahidahsaleh@gmail.com

[2] corresponding author: lan@usm.my

biomedical application [18]. From experimental work, gold nanoshells were grown on silica nanoshere have average diameter ranging from 40 to 180 nm. The changing in thickness of gold nanoshell by varying the amount of gold-decorated APTES-functionalized silica nanoparticles, the surface plasmon resonance of the silica gold nanoshells could be adjusted to any wavelength up to near infrared region which making them ideal for biomedical applications [29].

Well established theoretical tools are used to calculate the solution of Maxwell's equations for metallic nanoparticles surrounded in a dielectric environment to determine the particle plasmons. The discrete dipole approximation toolbox (DDSCATT) was designed for the simulation of scattering from interstellar graphite grains but has in recent years been widely used within the field of plasmonics. Also, there are other general simulation toolkit for the solution Maxwell's equations which is known as finite difference time domain (FDTD). In this paper, we use the simulation toolbox MNPBEM for metallic nanoparticles (MNP), developed by Garcia de Abajo and Howie which is based on a boundary element method (BEM) approach. Figure 1 shows simulation flow chart where parameter particle and dielectric will be define as we need. After that, the comparticle command will combine the parameters. As the excitation from the wavelength and the parameter, we can compute for BEM to find the solution of Maxwell's equation surface charge denote as sig. From the sig, measurement can be plotted as extinction, absorption or scattering efficiency against wavelength.

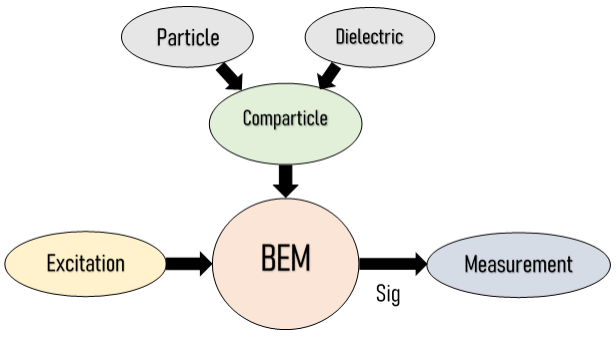


Figure 1. Flow chart of the calculation using boundary element method by MNPBEM toolbox [30]

As far as we know, this is the first reported treatment of FDTD and DDSCATT on Maxwell's equation using MNPBEM mode. By using this mode, calculation in complex interaction is faster, in order to produce comparable result to a more complicated mode. The MNPBEM method adopts a dielectric environment where bodies with homogeneous and isotropic dielectric functions are separated by abrupt interfaces, rather than allowing for a general inhomogeneous dielectric environment means that all the interactions between the gold nanoparticle and surrounding media is constant throughout the surface [30]. Tuned surface plasmon resonance wavelength position in the near-infrared region by using silica core gold nanoshells by either changing the core diameter and thickness or ratio (core: shell diameter) is demonstrated.

## II. CALCULATION METHOD

The plasmon resonance position wavelength and the magnitude of extinction efficiency are defined by electromagnetic boundary conditions at the inner-shell surface cavity and the outer-shell surface sphere. This definition is known as plasmon hybridization model [34]. In this work, the extinction efficiency spectrum of gold nanoshell of thickness t surrounding a dielectric core of diameter d was calculated in the visible—near-infrared region by deploying the Maxwell's equations solved using the boundary element method (BEM) [30], [32]. To solve full Maxwell's equations, the scalar and vector potentials are needed to fulfill a Helmholtz equation by defining a Green's function,

$$(\nabla^2 + k_i^2)G_i(\boldsymbol{r},\boldsymbol{r}') = -4\pi\delta(\boldsymbol{r}-\boldsymbol{r}'), \quad G_i(\boldsymbol{r},\boldsymbol{r}') = \frac{e^{ik_i|\boldsymbol{r}-\boldsymbol{r}'|}}{|\boldsymbol{r}-\boldsymbol{r}'|} \tag{1}$$

where $k_i$ is the wavenumber for medium $\mathbf{r}$.

$$\phi(\boldsymbol{r}) = \phi_{ext}(\boldsymbol{r}) + \oint_{V_i} G_i(\boldsymbol{r},\boldsymbol{s})\sigma_i(\boldsymbol{s})da \tag{2}$$

$$\boldsymbol{A}(\boldsymbol{r}) = \boldsymbol{A_{ext}}(\boldsymbol{r}) + \oint_{V_i} G_i(\boldsymbol{r},\boldsymbol{s})\boldsymbol{h_i}(\boldsymbol{s})da \tag{3}$$

The first derivative of the Green's function is considered in order to find the Helmholtz equations, the solution in equation (2,3) can determine the scalar and vector potentials from surface charge, $\sigma_i$ and current distribution, $\boldsymbol{h_i}$ that illustrate the external pertubation. From the BEM approach, the boundary integrals derived from equations (2, 3) are approximated by sums of boundary elements. The boundary calculations of full Maxwell's equations are lengthy equations. Thus, the surface charges and currents are calculated by matrix inversions and multiplications [30].

For the core of nanoparticle, we used a refractive index of 1.45 which corresponds to silica since silica is widely use in experimental work and it is biocompatible [17]. Gold nanoshell dielectric function is wavelength-dependent on complex refractive index of bulk gold [31]. The surrounding medium is liquid water with a refractive index of 1.33. The extinction efficiency spectrum was recorded in the visible—near-infrared region from 400 to 1000 nm [32]. In this work, we also study the correlation between surrounding medium refractive index and plasmon resonance position of silica-core—gold-nanoshell spectra and also the role of fixed total nanoparticle size. Refractive index for human blood plasma and liver tissue were assumed to be 1.351 and 1.3748 respectively [33, 34].

Table 1. The parameter use in this simulation

| | **Simulation parameter** | Ref. |
|---|---|---|
| **Refractive index of silica core** | n = 1.45 | |
| **Dielectric function of gold** | Calculated by Johnson and Christy | [31] |
| **Refractive index of surrounding medium** | n = 1.33 (water)<br>n = 1.351 (human blood plasma)<br>n = 1.3748 (liver tissue) | [33], [34] |
| **Different silica core diameter** | d = 20, 40, 60, 80 and 100 nm | |
| **Different gold nanoshell thickness** | t = 5, 10, 20, 40, and 60 nm | |
| **Different silica to gold nanoshell ratio radius** | 0.5, 1.5, 3.5, 7.5, and 15.5 | |

## III. RESULTS AND DISCUSSION

Figure 2 shows the calculated spectra of the extinction efficiency for silica—gold nanoshell with fixed thickness of gold nanoshell at t = 5 nm and different diameter of silica core d = 20, 40, 60, 80, and 100 nm. From here we can compare the behaviour of each thickness in different core diameter in order to understand the effect of silica core diameter encapsulated by gold nanoshell. In the case of core and nanoshell system simulation, we observed that there are at least two resonances for a larger core diameter which corresponds to the excitation of the surface plasmon polaritons [32], [35]. Data from Figure 2 also indicates that, the plasmon resonance redshifted by increasing the core size and with the appearance of small shoulder, most likely due to the quadrupole resonance at larger core [31], [36]. The coupling resonance is the highest peak which is due to dipole resonance [35]. At 80 nm and 100 nm diameter of silica core, the small shoulder is observed around 690 nm and 730 nm respectively, which corresponds to the quadrupole resonance mode [36].

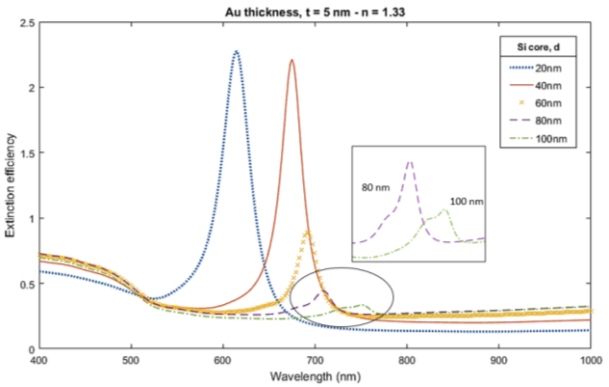


Figure 2. Calculated extinction efficiency spectra with varying the core. Five different core sizes (d = 20, 40, 60, 80 and 100 nm) with t = 5 nm nanoshell thickness. Inset is the curves profile in circled area

Figure 3 shows the result of fixed core diameter (d = 40 nm) in order to observe the different thickness of gold nanoshell. For spectra A, we calculated for different thickness t = 5, 10, 20, 40 and 60 nm with fixed silica core diameter d = 40 nm. The wavelength position is redshifted when we decreased the thickness of gold nanoshell from 5 nm to 60 nm. From here we can see that gold with nanoshell thickness of t = 10 nm is the highest in extinction efficiency value. The peculiar fluctuation of extinction efficiency with small full-width-half-maximum (FWHM) for t = 5 and 10 nm deserve further scrutiny. As such, spectra B of different thickness t = 2, 4, 6, 8, and 10 nm with silica core diameter fixed value which d = 40 nm was calculated. From this data, we can see that the surface plasmon resonance wavelength

position is redshifted when the thickness of gold nanoshell decrease. From these observation, the good thickness which having the optimum surface plasmon wavelength position and highest in extinction value is at gold nanoshell thickness t = 8 nm. The broadening of the plasmon resonance wavelength is due to the collision of conduction band electrons with the particle surface become important at thinnest gold nanoshell [37].

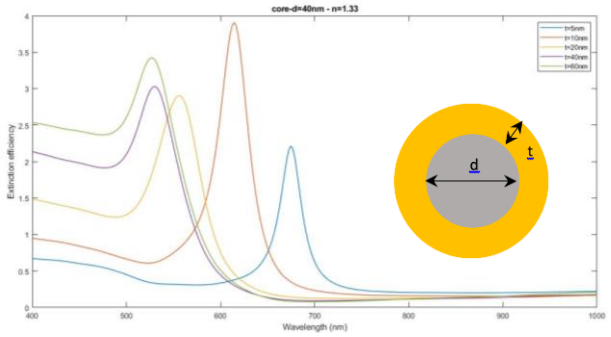


(a)

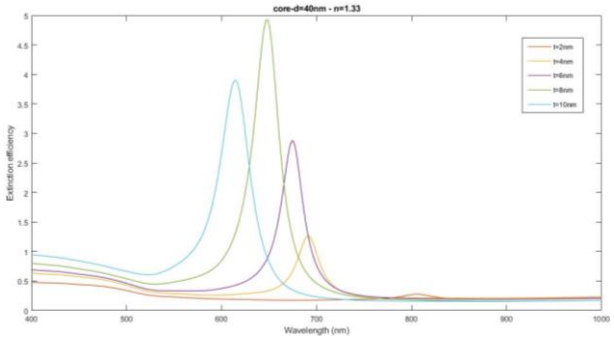


(b)

Figure 3. Calculated extinction efficiency spectra with varying nanoshell thickness. Spectra (a) for five different thickness (t = 5, 10, 20, 40, 60 nm) with fixed core diameter (d = 40 nm). Spectra (b) for five different thickness extended from spectra A to see the increment between 5 to 10 nm (t = 2, 4, 6, 8, 10 nm) with fixed core diameter (d = 40 nm)

Figure 4 shows the relation of the core to thickness ratio of the silica core and gold nanoshell in the different dielectric medium. The shifting of surface plasmon resonance occurs in the dielectric medium is due to the polarization of the dielectric between the core and the inner shell, the outer shell and embedded surrounding medium [32], [37]. From the data in Figure 3, there is no significant change in surface plasmon wavelength position when we changed the surrounding medium to the refractive index of human blood plasma (1.351) and liver tissue (1.3748) as observed experimentally by other worker [33], [34]. However, there is an increasing in trend on the plasmon resonance position when we increase the thickness ratio. This results can be explained clearly by using the plasmon hybridization model, which explain the physical origin of the tuneable plasmon resonance in metal nanoshell [36], [38]. For this observation, a possible description is offered. First, the nanoshell is a two-interface system where they support two distinct plasmon modes: an outer shell-surface sphere mode and an inner shell surface cavity mode, which will hybridize with each other and lead to a splitting into two modes. Then, a thinner shell ensures stronger near-field coupling and the larger core contribute to a larger polarization, therefore leading to a larger plasmon resonance shift. For, a smaller total size, there is no coupling resonance due to the role of total nanoparticle size in determining the plasmon resonance position. Finally, the highest ratio lies in the near-infrared region, where biological tissues transmissivity is the highest and away from the haemoglobin visible absorption around 500-600 nm. Therefore, the nanoshells scheme are much more suited to in-vivo imaging and therapy applications as compared to the gold nanospheres [39].

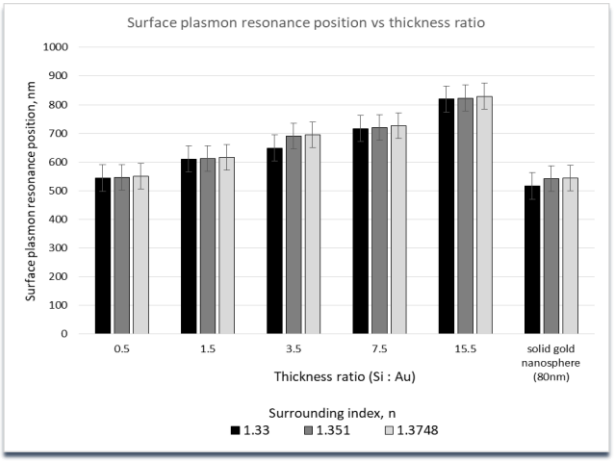


Figure 4. Comparison between the ratio of the thickness of nanoshell and core versus plasmon resonance red and blue shift

## IV. CONCLUSION

From this work, we demonstrated the role of core size for nanostructures and showed a good agreement for plasmon resonance position when the silica core diameter are 20 nm

and 40 nm. The role of gold nanoshell thickness also shows a good agreement for plasmon resonance position when the gold nanoshell thickness is at t = 8 nm which gives the highest extinction efficiency value. However, in different core—nanoshell ratio, the plasmon resonance position is redshifted to a near-infrared region when the ratio of core—nanoshell decrease but did not show any significant change in different medium. From these observation, the role of the core—nanoshell ratio shows that the surface plasmon resonance position is depends on the different ratio but it works independently on the different surrounding medium. It has also been observed that for large silica core diameter, the coupling resonance occurs between the inner shell cavity mode and the outer shell sphere mode. Therefore, the plasmon resonance position can be tuned to near-infrared region by changing the parameter of silica core gold nanoshell. Hence, the agreement of simulation work can be as aid for the selection of nanoparticles for specific biomedical application since the silica core gold nanoshell is extremely difficult to be characterize experimentally.

## V. ACKNOWLEDGEMENT

The authors would like to thank Ministry of Higher Education and Universiti Sains Malaysia for funding this research work through TRGS Grant (203/PFIZIK/6763003).

## VI. REFEREENCES

[1] Mcconnell, WP, Novak, JP, Rousseau iii, LC, Fuierer, RR, Tenent, RC & Feldheim, DL 2000, 'Electronic and optical properties of chemically modified metal nanoparticles and molecularly bridged nanoparticle arrays', *J. Phys. Chem. B*, vol. 104, no. 38, pp. 8925–8930.

[2] Scaletti, F, Soo, C, Messori, L & Rotello, VM 2014, 'Rapid purification of gold nanorods for biomedical applications', *MethodsX*, vol. 1, pp. 118–123.

[3] Faraday, M 1897, 'X. The Bakerian Lecture. – Experimental relations of gold (and other metals) to light', *Philos. Trans. R. Soc. London*, vol. 147, pp. 145–181.

[4] Schejn, A, Ott, M, Dabert, M, Vidal, L & Balan, L 2018, 'Photo-induced design of re fl ective metallized gold @ polymer coatings with tuned architecture', Mater. *Des*. vol. 160, pp. 74–83.

[5] Bonyár, A *et al.* 2018, 'Investigation of the performance of thermally generated gold nanoislands for LSPR and SERS applications', *Sensors Actuators B. Chem.*, vol. 255, pp. 433–439.

[6] Rossi, G & Monticelli, L 2016, 'Gold nanoparticles in model biological membranes: A computational perspective', *Biochim. Biophys. Acta*, vol. 1858, no. 10, pp. 2380–2389.

[7] Qin, H *et al.* 2017, 'Dynamic Au-Thiolate interaction induced rapid self-healing nanocomposite hydrogels with remarkable mechanical behaviors', *CHEM*, vol. 3, no. 4, pp. 691–705.

[8] Rajeshkumar, S 2016, 'Anticancer activity of eco-friendly gold nanoparticles against lung and liver cancer cells', *J. Genet. Eng. Biotechnology*, vol. 14, no. 1, pp. 195–202.

[9] Ul, N *et al.* 2015, 'Green synthesis and biological activities of gold nanoparticles functionalized with Salix Alba', *Arab. J. Chem.*, pp. 1878–5352.

[10] Xu, C *et al.* 2018, 'Bacteria-like mesoporous silica-coated gold nanorods for positron emission tomography and photoacoustic imaging-guided chemo-photothermal combined therapy', *Biomaterials*, vol. 165, pp. 56–65.

[11] Nasrin, F *et al.* 2018, 'Single-step detection of norovirus tuning localized surface plasmon resonance-induced optical signal between gold nanoparticles and quantum dots', *Biosens.*

*Bioelectron*.

[12] Liu, R, Wang, Q, Li, Q, Yang, X, Wang, K & Nie, W 2017, 'Surface plasmon resonance biosensor for sensitive detection of microRNA and cancer cell using multiple signal amplification strategy', *Biosens. Bioelectron.*, vol. 87, pp. 433–438.

[13] Li, M, Wu, D, Chen, Y, Shan, G & Liu, Y 2019, 'Apoferritin nanocages with Au nanoshell coating as drug carrier for multistimuli-responsive drug release', *Mater. Sci. Eng. C*, vol. 95, pp. 11–18.

[14] Mei, Z, Dhanale, A, Gangaharan, A & Kumar, D 2016, 'Water dispersion of magnetic nanoparticles with selective Biofunctionality for enhanced plasmonic biosensing', *Talanta*, vol. 151, pp. 23–29.

[15] Tang, J, Fu, X, Ou, Q & Gao, K 2018, 'Hydroxide assisted synthesis of monodisperse and biocompatible gold nanoparticles with dextran', *Materials Science and Engineering C*, vol. 93, pp. 759-767.

[16] Dhamecha, D, Jalalpure, S & Jadhav, K 2015, 'Doxorubicin-functionalized gold nanoparticles: characterization and activity against human cancer cell lines', *Process Biochemistry,* vol.50, pp. 2298-2306.

[17] Zhao, X, Huang, Q & Jin, Y 2015, 'Gold nanorod delivery of LSD1 siRNA induces human mesenchymal stem cell differentiation', *Materials Science and Engineering C*, vol. 54, pp. 142–149.

[18] Baruah, D, Goswami, M, Narayan, RS Yadav, Yadav, A & Das, AM 2018, 'Biogenic synthesis of gold nanoparticles and their application in photocatalytic degradation of toxic dyes', *Journal of Photochemistry and Photobiology B: Biology,* vol. 186, pp. 51-58.

[19] Islam, NU, Jalil, K, Shahid, M & Muhammad, N 2015, 'Pistacia integerrima gall extract mediated green synthesis of gold nanoparticles and their biological activities', *Arabian Journal of Chemistry*, vol 117, doi: 10.1016/j.arabjc.2015.02.014.

[20] Hossen, N, Khalek, A, Chakma, S, Paul, BK & Ahmed, K 2018, 'Design and analysis of biosensor based on surface plasmon resonance', *Sensing and Bio-Sensing Research,* vol. 21, pp. 1-6.

[21] Liu, J *et al.* 2018, 'Recent advances of plasmonic nanoparticles and their applications', *Materials (Basel).*, vol. 11, no. 1833, pp. 1–21.

[22] Liu, B, Lu, Y, Yang, X & Yao, J 2017, 'Surface plasmon resonance sensor based on photonic crystal fiber filled with gold – silica – gold multilayer nanoshells', *Optics Communications*, vol. 405, pp. 281–287.

[23] Li, S *et al.* 2017, 'A sensitive SPR biosensor based on hollow gold nanospheres and improved sandwich assay with PDA-Ag@Fe3O4/rGO', *Talanta*, vol. 180, pp. 156-161.

[24] Lee, SY, Kim, GW & Ha, JW 2017, 'Differential interference contrast microscopy imaging of single gold nanospheres beyond the quasi-static limit', *Chemical Physics Letters,* vol. 676, pp. 108-111.

[25] Raliya, R, Davis, JT, Chaval-, S, Wang, W, Ravi, N & Biswas, P 2016, 'Biocompatibility of gold nanoparticles in retinal pigment epithelial cell line', *Toxicology in Vitro,* vol. 37, pp. 61-69.

[26] Tang, J *et al. 2018*, 'Calculation extinction cross sections and molar attenuation coefficient of small gold nanoparticles and experimental observation of their UV–vis spectral properties', *Spectrochimica Acta Part A Molecular and Biomolecular Spectroscopy*, vol. 191, pp. 513–520.

[27] Chen, Q, Ren, Y, Qi, H & Ruan, L 2018, 'Influence of PEG coating on optical and thermal response of gold nanoshperes and

nanorods', *Journal of Quantitative Spectroscopy and Radiative Transfer*, vol. 212, pp. 1-9.

[28] Billen, A, de Cattelle, A, Jochum, JK, Van Bael, MJ, Billen, J, Seo, JW, Brullot, W, Koeckelberghs, G & Verbiest, T 2019, 'Novel synthesis of superparamagnetic plasmonic core-shell iron oxide-gold nanoparticles', *Physica B: Condensed Matter,* vol. 560, pp. 85-90.

[29] Lien, TH, Le, TN, Do, TH, D, TT, Vu, Do, QH & Tran, HN 2013, 'Preparation and characterization of silica – gold core – shell nanoparticles', *Journal of Nanoparticle Research*, vol. 15, pp. 2091.

[30] Hohenester, U & Trügler, A 2012, 'MNPBEM - A Matlab toolbox for the simulation of plasmonic nanoparticles', *Computer Physics Communications*, vol. 183, no. 2, pp. 370–381.

[31] Johnson, PB & Christy, RW 1972, 'Optical constants of the noble metals', *Physical Review B,* vol. 6, no. 12, pp. 4370–4379.

[32] Quinten, M 2011, '*Optical properties of nanoparticle systems : Mie and beyond*', Wiley-VCH Verlag GmbH & Co. KGaA, Singapore.

[33] Reddy, NM, Kothandan, D, S. C. Lingam, SC & Ahmad, A 2012, 'A study on Refractive index of plasma of blood of patients suffering from Tuberculosis', *International Journal of Innovative Technology and Creative Engineering*, vol. 2, no. 8, pp. 23–25.

[34] Giannios, P *et al.* 2016, 'Visible to near-infrared refractive properties of freshly-excised human-liver tissues : marking hepatic malignancies', *Scientific Reports*, no. 6, pp. 27910.

[35] Oldenburg, SJ *et al.* 1999, 'Infrared extinction properties of gold nanoshells Infrared extinction properties of gold nanoshells', *Applied Physics Letters*, no. 75, pp. 2897–2899.

[36] Jain, PK & El-sayed, MA 2007, 'Universal scaling of plasmon coupling in metal nanostructures : Extension from particle pairs to nanoshells', *Nano Letters*, vol. 7, no. 9, pp. 2854–2858.

[37] Mehrdel, B, Aziz, AA & Yoon, TL 2017, 'Resonance position and extinction efficiency of a single silica coated gold nanoshell when size effects of core is matter', *AIP Conference Proceedings,* vol. 1838, no. 1, pp. 020012.

[38] Prodan, E, Radloff, C, Halas, NJ & Nordlander, P 2003, 'A hybridization model for the plasmon response of complex nanostructures', *Science,* vol. 302, no. 5644, pp. 419-22.

[39] Jain, PK, Lee, KS, El-sayed, IH & El-sayed, MA 2006, 'Calculated absorption and scattering properties of gold nanoparticles of different size , shape and composition : Applications in biological imaging and biomedicine', *The Journal of Physical Chemistry B*, vol. 110, no. 14, pp. 7238–7248.